MATEC Web of Conferences **137**, 04002 (2017) DOI: 10.1051/matecconf/201713704002
MTeM - AMaTUC 2017

Inference of power loss in spherical joints of the 6RSS parallel mechanism

Lucian Milica[1,*] and *Gabriel* Andrei[1]
[1]"Dunarea de Jos" University, Department Mechanical Engineering, 800201 Galati, Romania

Abstract. This paper presents an analysis of the power losses due to the friction between the components of the spherical joints, belonging to a 6RSS parallel mechanism. The determination of power losses in spherical joints has been done with an application where the characteristic point follows a closed space curve. The trajectory of the point on the convex semicuple in contact with the concave semicuple it has been determined by using facilities of the CATIA software.

1 Introduction

The paper presents a method for determining the power losses for a parallel mechanism by friction between the components of the spherical joints that form its six kinematic chains. Spherical joints are a special category of joints with the particularity that the contact surfaces are spherical, with or without lubricant between them.

The importance of spherical joints has led many researchers to carry out numerous studies to determine their influence on the dynamics of mechanical systems [1-4]. The contact forces acting in such joints are of a particular importance in the design and analysis of spherical joints [5-7]. It was also analyzed, based on contact forces, the energy dissipated in a spherical joint [8,9].

Recent studies have analyzed how the contact forces within the spherical joints that form space structures affect their stability and precision [10-12].

Liu et al. [13] have developed a mathematical model for approximation of the dimensional tolerance of a spherical joint which is based on distributed elastic forces.

2 Geometrical modeling of the spherical joint

Let us consider a kinematic chain of a 6RSS parallel mechanism (Figure 1). The kinematic chain is composed of rotational joints in the points O_k and spherical joints in the points A_k and B_k, respectively. The actuating arms $a_k = O_k A_k = 254$ mm are rotated at an angle θ_k around the axis passing through the O_k point, by means of actuators mounted on the base plate. The position of the O_k point relative to the $\{R\}$ system, the length of the actuating arms k and the value of the angle θ_k are known. In Figure 2, has been shown the position of the O_k points.

* Corresponding author: milica.lucian@ugal.ro

Also, it has been noted with $e = 106$ mm the apothem of the base and with $g = 76$ mm the distance O_kO_{k+1} which is the same distance as B_kB_{k+1}.

Let's look at one of the six kinematic chains of the 6RSS parallel mechanism (Figure 3). The degree of mobility of the mechanism is given by the Grübler-Kutzbach formula:

$$M = 6 \cdot m - \sum_{n=1}^{5} c \cdot k_n = 6 \cdot 13 - (6 \cdot 5 + 12 \cdot 3) = 12 \quad (1)$$

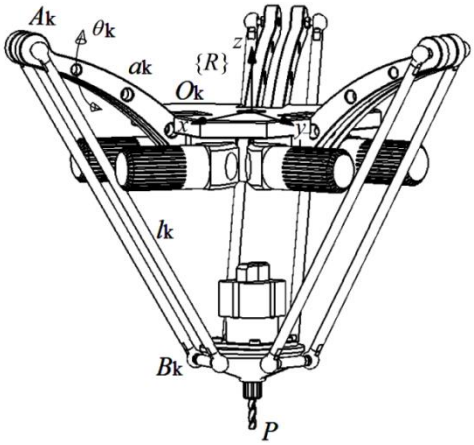

Fig. 1. Highlighting the O_k, A_k, r_k, θ_k parameters of the new 6RSS parallel manipulator.

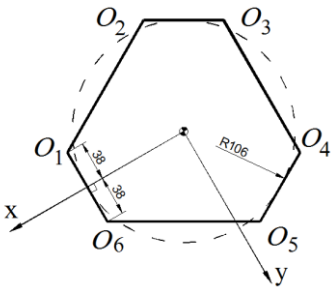

Fig. 2. The position of the O_k centers of the rotational joints.

Each actuating arm has a local mobility given by the rotation around the A_kB_k axis, independent motion relative to the other possible motions of the mechanism. Eliminating these six isolated mobilities it results $M = 6$.

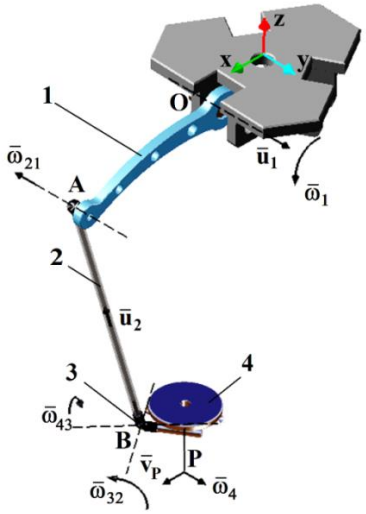

Fig. 3. Representation of a kinematic chain of the mechanism.

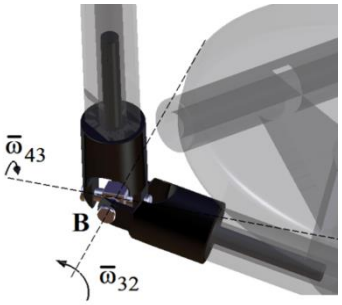

Fig. 4. Highlighting the 4^{th} degree kinematic joint for the B point.

In the analysis of mobility it has been defined the following parameters:
- $m = n + 1$ (m represents the number of mobile kinematic elements);
- c is the class of the kinematic joints;
- k_n is the number of kinematic joints of class n.

For a more intuitive representation, it has been replaced the spherical joint from point *B* with a U-joint. This modification does not affect the degree of mobility of the mechanism. The direct kinematic model involves determining the speed of point *P*, based on six systems of equations, one for each kinematic chain (2):

$$S = \begin{cases} \boldsymbol{\omega_1} \times \mathbf{OP} + \boldsymbol{\omega}_{21} \times \mathbf{AP} + \boldsymbol{\omega}_{32} \times \mathbf{BP} + \boldsymbol{\omega_{43}} \times \mathbf{BP} = \mathbf{v_P} \\ \boldsymbol{\omega_1} + \boldsymbol{\omega}_{21} + \boldsymbol{\omega}_{32} + \boldsymbol{\omega_{43}} = \boldsymbol{\omega_4} (\boldsymbol{\omega_4} \equiv \boldsymbol{\omega_P}) \end{cases} \quad (2)$$

The variables in this case are: ω_1, ω_{32}, ω_{43}, $\boldsymbol{\omega}_{21}$, $\boldsymbol{\omega}_4$, $\mathbf{v_P}$.

Using the inverse kinematic model in which is known the linear speed ($\mathbf{v_P}$) and the angular speed ($\boldsymbol{\omega}_4 \equiv \boldsymbol{\omega_P}$) of point *P*, it can be determined six scalar variables: ω_1, ω_{32}, ω_{43}, ω_{21}^x, ω_{21}^y, ω_{21}^z.

3 Application for the inverse kinematic model

Let's look at the spherical joint of one of the points A_k.

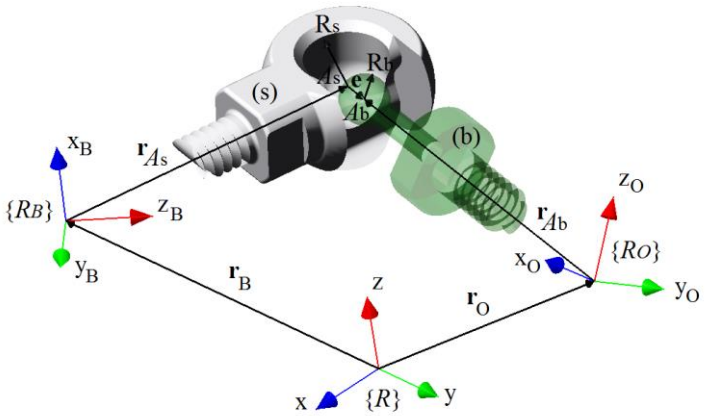

Fig. 5. Representing spherical joint with point position A_s and A_b.

Let's consider two bodies b (ball) and s (socket) that represent the spherical part and the concave part of a spherical joint from point A_1 (Figure 5).

The spherical part of the body b is inside the concave part of the body s. It will be noted with $\mathrm{R_s}$ and $\mathrm{R_b}$ the radius of the spherical body b and the concave body s. The difference between the radius $\mathrm{R_s}$ and $\mathrm{R_b}$ is the radial tolerance denoted by $j = \mathrm{R_s} - \mathrm{R_b}$ expressed in the above figure by the vector $\mathbf{e}$. The orientation of this vector coincides with the one of the axis passing through the points A_s and A_b, identical to the axis of the body b.

The position of the point A_s in the system $\{R_B\}$ is given by the position vector $\mathbf{r_{A_s}}$ and the position of the point A_b in the system $\{R_O\}$ by the position vector $\mathbf{r_{A_b}}$. Also, $\mathbf{r_B}$ and $\mathbf{r_O}$ are positional vectors of system origin $\{R_B\}$ and $\{R_O\}$ respectively. Norm of the vector $\mathbf{e}$ in the global system $\{R\}$ is:

$$|\mathbf{e}| = \sqrt{(x_A^b - x_A^s)^2 + (y_A^b - y_A^s)^2 + (z_A^b - z_A^s)^2} \quad (3)$$

It has been done an application in which was considered the characteristic point *P* in motion on a spatial curve of length $\mathrm{L} = 528.637$ mm, when $\beta \neq \gamma \neq 0 = ct$ and α is variable (α, β, γ are the three orientation parameters of the mobile platform). In this application, the point *P* is in permanent contact with the curve. It has been stated that in the

application done through the Catia software, the motion parameter is an arc of curve by equal length, dividing the curve into 72 equally distributed points on it, whose Cartesian coordinates are returned by the program.

The particularity of the application is that the inertia forces $\mathbf{F_i}$ are neglected, the motion being performed very slowly, therefore, there is only one axial force $\mathbf{F_{21}}$ acting in the **AB** direction.

Due to the imposed initial condition - the force acts in the **AB** direction - the eccentricity **e** is manifested in this direction throughout the motion. At the opposite pole of this eccentricity is the point of contact k between the spherical head and the concave part of the spherical joint (Figure 6).

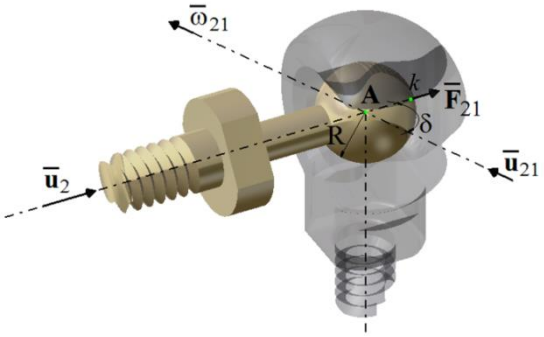

Fig. 6. Highlighting the point of contact k of the spherical joint *A*.

It has been noted with δ the angle between versor $\mathbf{u_2}$ and the versor $\mathbf{u_{21}}$ and with R the radius of the spherical head of the joint. Also $\boldsymbol{\omega}_{\mathbf{21}}$ is the angular velocity of the contact point k.

Taking into account the imposed condition $\mathbf{F_i} = 0$, it can be written the following expression for the power loss $\mathbf{P_f}$ determinated by friction between the kinematic joint elements in point *A*:

$$\mathbf{P_f} = \mu \cdot \mathbf{F_{21}} \cdot \boldsymbol{\omega}_{\mathbf{21}} \cdot \mathrm{R} \cdot \sin\delta \tag{4}$$

The mechanical work of friction forces is:

$$\mathbf{L_f} = \int_0^{\mathrm{T}} \mathbf{P_f}\,\mathrm{dt} = \mu \cdot \mathbf{F_{21}} \cdot \mathrm{R} \int_0^{\mathrm{T}} (\boldsymbol{\omega}_{\mathbf{21}} \cdot \sin\delta)\,\mathrm{dt} \tag{5}$$

It can be considered the axial force $\mathbf{F_{21}}$ constant and unitary ($\mathbf{F_{21}} = \mathrm{ct} = 1$) throughout the entire during movement.

The value of the angle δ is given by the expression:

$$\cos\delta = \frac{\mathbf{u_2}\cdot\boldsymbol{\omega_{21}}}{|\mathbf{u_2}|\cdot|\boldsymbol{\omega_{21}}|} \rightarrow \sin\delta = \sqrt{1-\cos^2\delta} \tag{6}$$

Based on of the Catia software, it can be determined the components of the vector $\boldsymbol{\omega}_{\mathbf{21}}$, on the three directions (ω_{21}^x, ω_{21}^y, ω_{21}^z). Also, it can be determined the components (u_2^x, u_2^y, u_2^z) of the $\mathbf{u_2}$ versor of the spherical head axis.

From the six scalar components is resulting (7) and (8):

$$|\boldsymbol{\omega}_{\mathbf{21}}| = \sqrt{{\omega_{21}^x}^2 + {\omega_{21}^y}^2 + {\omega_{21}^z}^2} \tag{7}$$

$$\mathbf{u_2} \cdot \boldsymbol{\omega}_{\mathbf{21}} = \omega_{21}^x \cdot u_2^x + \omega_{21}^y \cdot u_2^y + \omega_{21}^z \cdot u_2^z \tag{8}$$

The integration of formula (5) was done numerically with the trapeze method, using the finite formula:

$$\mathbf{L_f} \approx \mu \cdot \mathbf{F_{21}} \cdot \mathrm{R} \sum_{i=1}^{72} (\boldsymbol{\omega}_{\mathbf{21}} \cdot \sin\delta)_i \cdot \Delta t \tag{9}$$

where:

$$\Delta t = \frac{T}{72}\ \mathrm{s} \tag{10}$$

represents the time required to go through one of the 72 equal circle arcs.

Admitting a constant speed of motion of the point on the curve, $v = 10\ \mathrm{mm/s}$, and knowing its length (L), results the time T required for following the curve:

$$T = \frac{L}{v} = 52.8637\ \mathrm{s} \rightarrow \Delta t = 0.7342\ \mathrm{s} \tag{11}$$

In Figures 7 and 8 it has been represented the variation of vector components $\boldsymbol{\omega}_{\mathbf{21}}$ and $\mathbf{u_2}$ depending on the position of the P_j point on the curve.

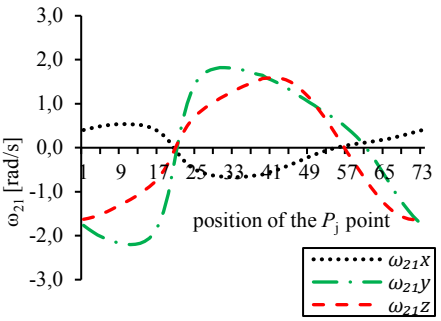

Fig. 7. Vector components $\boldsymbol{\omega}_{21}$ depending on the position of the P_j point.

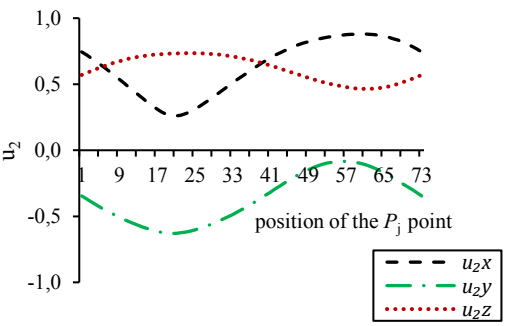

Fig. 8. Vector components $\mathbf{u}_2$, depending on the position of the P_j point.

By admitting a friction coefficient $\mu = 0.2$, from (4), (6), (7) and (8) it can be determined the lost power by friction $\mathbf{P_f}$ in the kinematic joint of point A for each position P_j of the characteristic point (Figure 9). By summing these values, it has been obtained the frictional power losses in the A kinematic joint, when the characteristic point follows the curve.

$$\mathbf{P_f} = \mu \cdot \mathrm{R} \sum_{i=1}^{72} (\boldsymbol{\omega}_{\mathbf{21}} \cdot \sin\delta)_i = 0.13\ \mathrm{W} \tag{12}$$

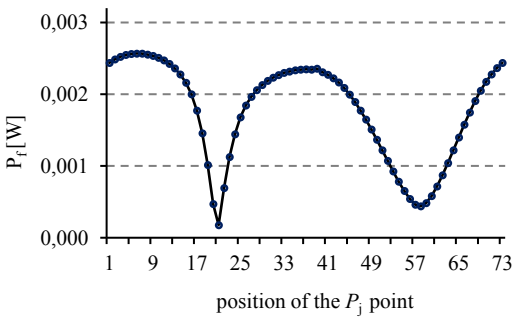

Fig. 9. Frictional power loss $\mathbf{P_f}$, for each position of the P_j characteristic point.

Also, it can be determined, using the functions of Catia software, the trajectory of a point k' belonging to the spherical head of the joint on its concave surface.

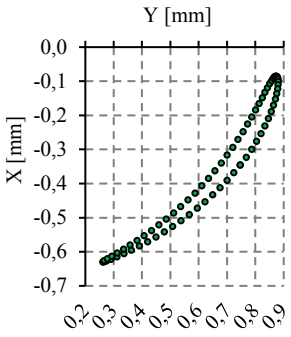

Fig. 10. Projection of the k' point trajectory on XY plane.

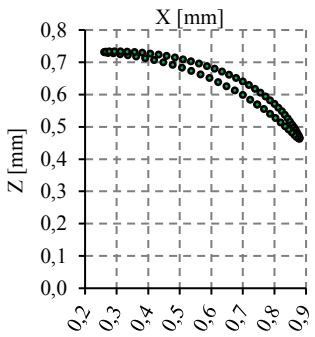

Fig. 11. Projection of the k' point trajectory on ZX plane.

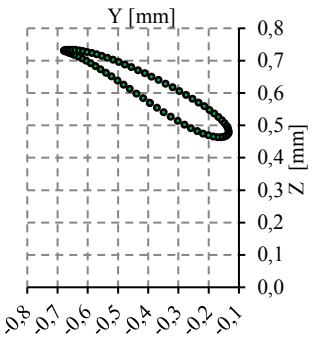

Fig. 12. Projection of the k' point trajectory on ZY plane.

Projecting the coordinates of these points on the three plans XY, XZ, ZY, it can be obtained the diagrams of Figures 10-12 which describe the trajectory of point k'.

4 Conclusions

This paper presents an original method for determining the power losses due to friction between the components of the spherical joints belonging to a 6RSS parallel mechanism.

The determination of these power losses in spherical joints was done in an application where, the characteristic point *P* follows a closed space curve, neglecting the inertial forces and the motion being very slow.

Using the Catia software, the variation graphs of the versor $\mathbf{u_2}$ of the direction **AB** and of the vector $\boldsymbol{\omega}_{21}$ have been determined depending on the position of the point P_j on the given spatial curve. The trajectory of a point belonging to the spherical head of the spherical kinematic joint of the parallel mechanism was obtained and the graphs of the traiectory's projections on the three plans XY, ZX, YZ were done.

References

1. S. Dubowsky, F. Freudenstein, ASME J. Eng. Ind., **93**, 305–309 (1971)
2. P. Flores, J. Ambrósio, J. P. Claro, H. M. Lankarani, C.S. Koshy, Mech. Mach. Theory, **41**, 247–261 (2006)
3. O.A. Bauchau, J. Rodriguez, Int. J. Solids Struct., **39**, 41–63 (2002)
4. P. Flores, Nonlinear Dyn., **61**, 633–653 (2010)
5. F. Farahanchi, S. W. Shaw, J. Sound Vib., **177**, 307–324 (1994)
6. G. S. Boltachev, N. B. Volkov and N. M. Zubarev, Int. J. Solids Struct., **49**, 2107-2114 (2012)
7. J. Rhee, A. Akay, Mech. Mach. Theory, **31**, 121–134 (1996)
8. P. Flores, J. Ambrósio, and J. P. Claro, Multibody Syst. Dyn., **12**, 47–74 (2004)
9. M. Lankarani, and P. E. Nikravesh, ASME J. Mech. Des., **112**, 369–376 (1990)
10. J. A. C. Ambrósio, NATO Adv. Sci. Inst., **2**, 15–33 (2002)
11. M. A. Brown, Adv. Space Res., **48**, 1747-1753 (2011)
12. Z. H. Qi, Y. S. Xu, X. M. Luo, and S. J. Yao, Multibody Syst. Dyn., **24**, 133-166 (2010)
13. C. S. Liu, K. Zhang, and L. Yang, J. Comput. Nonlin. Dyn., **1**, 160-167 (2006)